EFFECTS OF FLOW TOPOLOGY ON INERTIAL PARTICLE ACCELERATION

Juan P. L. C. Salazar, juan.salazar@ufsc.br
Centro de Engenharia da Mobilidade, Universidade Federal de Santa Catarina, Joinville, SC, 89218-000, Brazil
Programa de Pós-Graduação em Engenharia Mecânica, Universidade Federal de Santa Catarina, Florianópolis, SC, 88040-900, Brazil
Lance R. Collins, lc246@cornell.edu
Sibley School of Mechanical & Aerospace Engineering, Cornell University, Ithaca, NY, 14853, USA

Abstract. *Flow topology and its connection to acceleration of inertial particles is explored through invariants of the strain-rate and rotation-rate tensors. A semi-quantitative analysis is performed where we assess the contribution of specific flow topologies to acceleration moments. Our findings show that the contributions of regions of high vorticity and low strain decrease significantly with Stokes number, a non-dimensional measure of particle inertia. The contribution from regions of low vorticity and high strain exhibit a peak at a Stokes number of approximately 0.2. The results shown here have recently been published in [Salazar, J.P.L.C. and Collins, L.R., 2012. "Inertial particle acceleration statistics in turbulence: Effects of filtering, biased sampling, and flow topology'. Phys. Fluids, Vol. 24, p. 083302].*

Keywords:*Turbulence, Inertial Particle Acceleration, Flow Topology*

1. INTRODUCTION

Acceleration is the key input to the family of stochastic models that yield a one-time continuously differentiable velocity autocorrelation that attempts to capture the Reynolds number dependence of the Lagrangian velocity and acceleration (Pope, 2002). Because of the usefulness of stochastic equations in models for turbulent relative dispersion (Salazar and Collins, 2009) and Lagrangian probability density function (PDF) methods (Pope, 1994), a large number of direct numerical simulations (DNS) (Yeung *et al.*, 2006a,b, 2007) and experiments (Mordant *et al.*, 2004; Gylfason *et al.*, 2004; Xu and Bodenschatz, 2008; Brown *et al.*, 2009) have been devoted to the study of acceleration statistics of fluid tracers. Beginning with the work of Bec *et al.* (2006), acceleration statistics of inertial particles have been the focus of many recent DNS (Calzavarini *et al.*, 2009; Lavezzo *et al.*, 2010) and experiments (Gerashchenko *et al.*, 2008; Volk *et al.*, 2008; Qureshi *et al.*, 2008). The current work is intended to provide a better understanding of inertial particle acceleration, aiding the development of finite-inertia particle models.

Particle inertia is usually parameterized by the Stokes number, which for a particle of diameter d and density ρ_p embedded in a fluid of kinematic viscosity ν and density ρ is given by $St \equiv \tau_p/\tau_\eta$, where $\tau_p \equiv \frac{1}{18}\frac{\rho_p}{\rho}\frac{d^2}{\nu}$ is the particle relaxation time, $\tau_\eta \equiv \left(\nu^3/\langle\varepsilon\rangle\right)^{1/4}$ is the Kolmogorov timescale, the most relevant fluid time scale for particle clustering, and ε is the instantaneous, local turbulent kinetic energy dissipation rate.

We investigate the relationship between the acceleration magnitude and the local flow topology and Stokes number. We use invariant plots of the rotation-rate and strain-rate tensors to characterize flow topology, following the original work of Chong *et al.* (1990).

2. NUMERICAL METHODS

The pseudo-spectral DNS code we use is thoroughly described in Brucker *et al.* (2007). Of particular relevance to this study is the forcing scheme we use to obtain statistically stationary turbulence. Energy is injected in the two lowest wavenumbers at each time step, offsetting the losses in kinetic energy owing to viscous forces, such that the total kinetic energy remains constant throughout the simulation. Table 1 summarizes the main fluid statistics. The evolution equations for small inertial particles, $d/\eta \ll 1$, were derived in final form by Maxey and Riley (1983). For large particle to fluid

Table 1. Table of DNS flow statistics. The turbulent kinetic energy is given by $\int_0^{\kappa_{\max}} E(\kappa)d\kappa$, where $E(\kappa)$ is the energy spectrum function and $\kappa_{\max}$ is the largest resolved wavenumber. The longitudinal integral length scale is given by $L = \pi/(2u'^2)\int_0^{\kappa_{\max}} [E(\kappa)/\kappa]\, d\kappa$. The Taylor microscale Reynolds number is given by $R_\lambda = u'^2\sqrt{15/(\nu\langle\varepsilon\rangle)}$

Quantity	Units	Value
Reynolds number	—	120
Turbulent kinetic energy k	$[\mathrm{L}^2\mathrm{T}^{-2}]$	1.43
Turbulent intensity $u' = \sqrt{2/3k}$	$[\mathrm{LT}^{-1}]$	0.98
Turbulent energy dissipation rate ε	$[\mathrm{L}^2\mathrm{T}^{-3}]$	0.32
Longitudinal integral scale L	$[\mathrm{L}]$	1.44
Integral time scale $T = L/u'$	$[\mathrm{T}]$	1.48
Kolmogorov length scale η	$[\mathrm{L}]$	0.017
Kolmogorov time scale τ_η	$[\mathrm{T}]$	0.097
Kolmogorov velocity scale u_η	$[\mathrm{LT}^{-1}]$	0.175
Small scale resolution $\kappa_{\max}\eta$	–	2.0
Normalized simulation time T_{end}/T	–	22.0
Number of grid points N^3	–	256^3
Number of particles at each St	–	32,768

density ratios, $\beta \equiv \rho_p/\rho_f \gg 1$, effects of added mass can be neglected. We also neglect the Basset history term and Faxén corrections to Stoke's law. Because of the low mass and low volume fractions, two-way coupling and effects on the continuity equation are neglected, respectively. The inertial particle evolution equations for position and velocity are,

$$\frac{dX_i}{dt} = v_i \tag{1}$$

$$\frac{dv_i}{dt} = \frac{u_i(\mathbf{X}) - v_i}{\tau_p}\,, \tag{2}$$

where X_i is the particle position, v_i is the particle velocity and $u_i(\mathbf{X})$ is the fluid velocity evaluated at the particle position. Equations 1 and 2 are solved numerically using Heun's method (two-stage Runge-Kutta) with use of an integrating factor. The fluid velocity is interpolated at the particle position by an eighth-order Lagrangian polynomial. The following Stokes numbers are simulated: $St = 0.025,\ 0.05,\ 0.1,\ 0.2,\ 0.5,\ 1,\ 2$. The full velocity gradient tensor is computed and stored in addition to position and velocity vectors at an interval of approximately $0.1\tau_\eta$.

3. RESULTS

Flow topology can be characterized by invariant plots of the velocity-gradient tensor $A_{ij} = \partial u_i/\partial x_j$, the symmetric strain-rate tensor $S_{ij} = 1/2\,(A_{ij} + A_{ji})$ and the anti-symmetric deviatoric rotation-rate tensor $W_{ij} = 1/2\,(A_{ij} - A_{ji})$, where by definition $A_{ij} = S_{ij} + W_{ij}$. Detailed information on the subject can be found in previous work (Chong *et al.*, 1990; Cantwell, 1992; Soria *et al.*, 1994; da Silva and Pereira, 2008). Each of these tensors satisfies a characteristic polynomial of the form,

$$\lambda^3 + P\lambda^2 + Q\lambda + R = 0\,, \tag{3}$$

where λ are the eigenvalues and P, Q and R are the first, second and third tensor invariants respectively. For incompressible flows $P = -A_{ii} = -S_{ii} = 0$. In this study, we will be interested exclusively in the invariants Q_S and Q_W, given by,

$$Q_S = -\frac{1}{2}S_{ij}S_{ij} = -\frac{1}{2}S^2\,, \tag{4}$$

$$Q_W = \frac{1}{2}W_{ij}W_{ij} = -\frac{1}{2}W^2\,. \tag{5}$$

The physical interpretation of these tensor invariants and classification of flows based on their values is described in the aforementioned literature. The invariants are commonly presented in the form of joint PDFs.

In order to understand how inertial particle acceleration relates to flow topology, in particular the acceleration magnitude and its higher order moments, we associate a given acceleration event to a position in the $(Q_W, -Q_S)$ plane. This procedure leads to the acceleration magnitude contour plots shown in Figure 1. The main effect of inertia is to stretch the isocontours of acceleration magnitude towards larger values of Q_W. This effect becomes quite significant for $St > 0.2$. With increasing St, in the limit of $Q_S \to 0$, a given value of $|a|$ is attained at a much larger value of Q_W than would be required for Q_S in the limit of $Q_W \to 0$. This trend is consistent with the notion that high-inertia particles are less susceptible to vortex trapping. We also observe a region in the $(Q_W, -Q_S)$ plane where the acceleration magnitude is approximately independent of Q_W. We reason that a possible cause for this is that as the particle inertia increases, the persistence of strain as seen by the inertial particle becomes larger than that of rotation (not shown), allowing the inertial particle more time to be influenced by strain than by rotation, therefore the observed behavior.

Although the conditional average of acceleration magnitude provides an interesting view of how acceleration relates to flow topology, it must be viewed in conjunction with the $(Q_W, -Q_S)$ joint PDFs shown in Figure 2. A certain value of $(Q_W, -Q_S)$ may be associated with a large acceleration event, however the probability of that event may be very low, such that the overall contribution to the variance and higher-order moments is not significant. The converse is also true. From Figure 2, we see that increasing inertia leads to a reduction in the asymmetry of the PDF. This effect peaks at $St \approx 0.5$ and then the asymmetry increases at larger St. This trend more or less coincides with the peak in particle clustering (Sundaram and Collins, 1997) and is consistent with the ejection of low St particles from regions of large Q_W. In Figures 1 and 2 we have identified four regions, where each corresponds to a particular flow topology. We assess the contribution of each of these regions to acceleration variance and higher-order moments through the following expression

$$\begin{aligned}\Lambda_p =& \frac{\langle [a_i a_i]^p \left| Q_W^U \le Q_W \le Q_W^L,\ -Q_S^L \le -Q_S \le -Q_S^U \right\rangle}{\langle [a_i a_i]^p \rangle} \\ =& \frac{\int_{Q_W^U}^{Q_W^L} \int_{-Q_S^L}^{-Q_S^U} g_p(Q_W, -Q_S) f(Q_W, -Q_S) dQ_W (-dQ_S)}{\int_0^\infty \int_0^\infty g_p(Q_W, -Q_S) f(Q_W, -Q_S) dQ_W (-dQ_S)} \,, \end{aligned} \tag{6}$$

where $g_p(Q_W, -Q_S)$ is the value of $[a_i a_i]^p$ evaluated at $(Q_W, -Q_S)$, $f(Q_W, -Q_S)$ is the joint PDF, Q_W^U, Q_W^L, $-Q_S^U$, $-Q_S^L$ delimitate the lower (L) and upper bounds (U) of the region of interest in the $(Q_W, -Q_S)$ plane and p is a non-negative integer. The computed values for Λ_p are shown in Figure 3. The region labeled as "1" corresponds to high Q_W and low $-Q_S$ events, which resemble solid body rotation. For fluid tracers ($St = 0$) the contribution of this region exceeds that of the region labeled as "2", of low Q_W and high $-Q_S$, associated with intense dissipation events. However, as St increases, region "1" contributes less towards $\langle [a_i a_i^p] \rangle$, attaining a minimum at $0.5 \le St \le 1$, coinciding with the peak in clustering at $St \approx 0.7$ (Sundaram and Collins, 1997). The region labeled as "4", of low Q_W and low $-Q_S$, dominates for moments $p \le 4$ at all St. Note that this is also the region with the smallest area in the $(Q_W, -Q_S)$ plane. For $p > 2$ and low St this region contributes less to the total moment than the other regions. The contribution of region "3", of high Q_W and high $-Q_S$ exhibits less St dependence than other regions and is more or less of similar magnitude for all values of p. Region "2" shows a peak at low St. We believe this is related to the accumulation of these particles in regions of high strain and low rotation, as can be seen in Figure 2, combined with the higher acceleration events associated with this region for $0 < St \le 0.5$. In addition, a careful analysis of Figure 2 reveals that with increasing inertia particles are ejected from regions of overlapping high strain and high rotation, while there is an increase in the number of particles in regions of high strain and low rotation. This suggests that low inertia particles are ejected not only from regions of high rotation, but also from regions of high strain. The analysis performed here is of a semi-quantitative nature, in that other regions could have been chosen and the statistical convergence of the moments $p > 2$ is not as good.

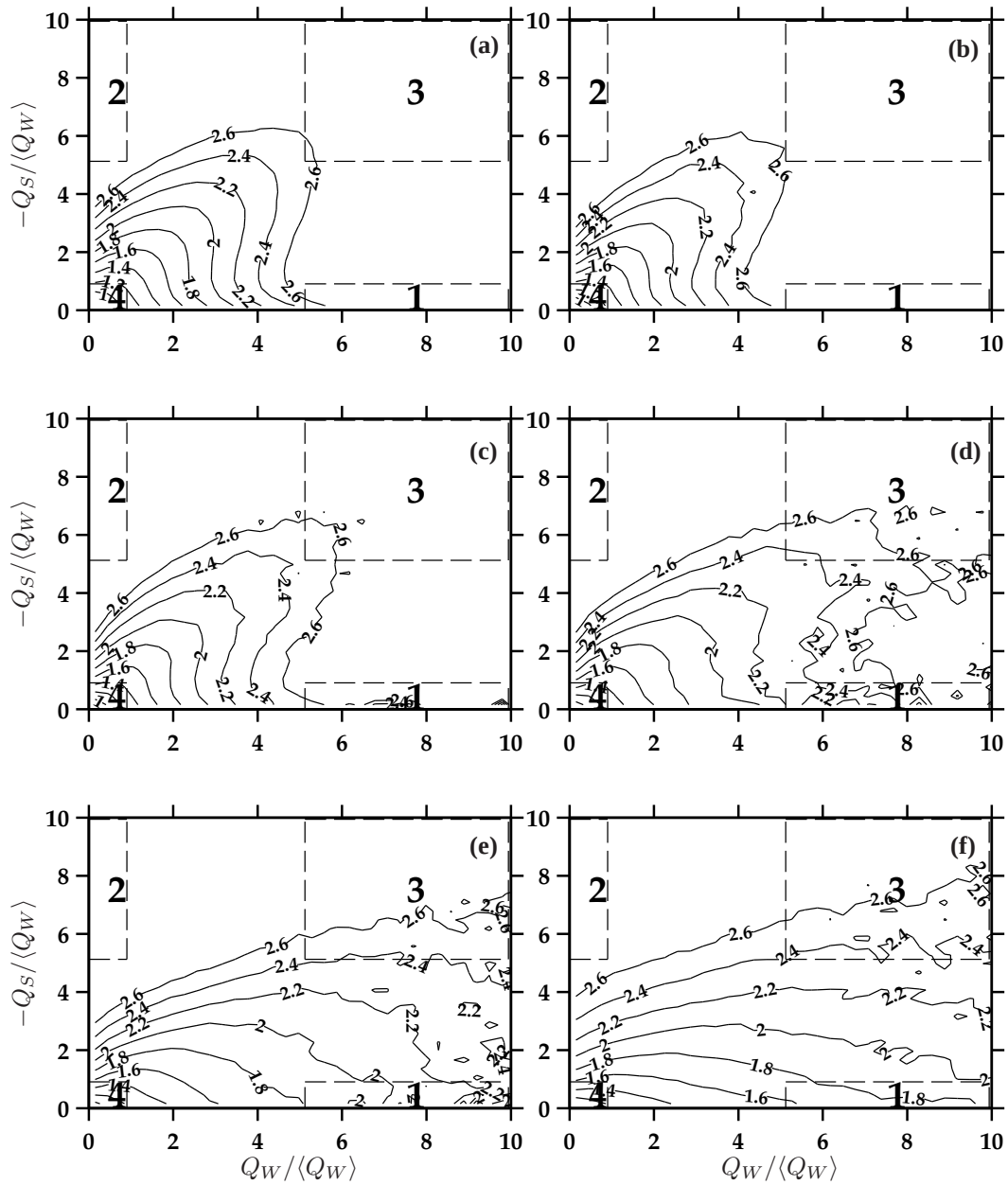

Figure 1. Conditional average of acceleration magnitude $|a|/a_{\text{rms}}(St)$ on the $(Q_W, -Q_S)$ invariant plane for (a) $St = 0.0$, (b) $St = 0.1$, (c) $St = 0.2$, (d) $St = 0.5$, (e) $St = 1$, and (f) $St = 2$. The areas outlied by dashed lines correspond to 1 - high Q_W and low Q_S, 2 - high Q_S and low Q_W, 3 - high Q_W and high Q_S, and 4 - low Q_W and low Q_S. The values for the ratio $|a|/a_{\text{rms}}(St)$ are indicated on the contour lines.

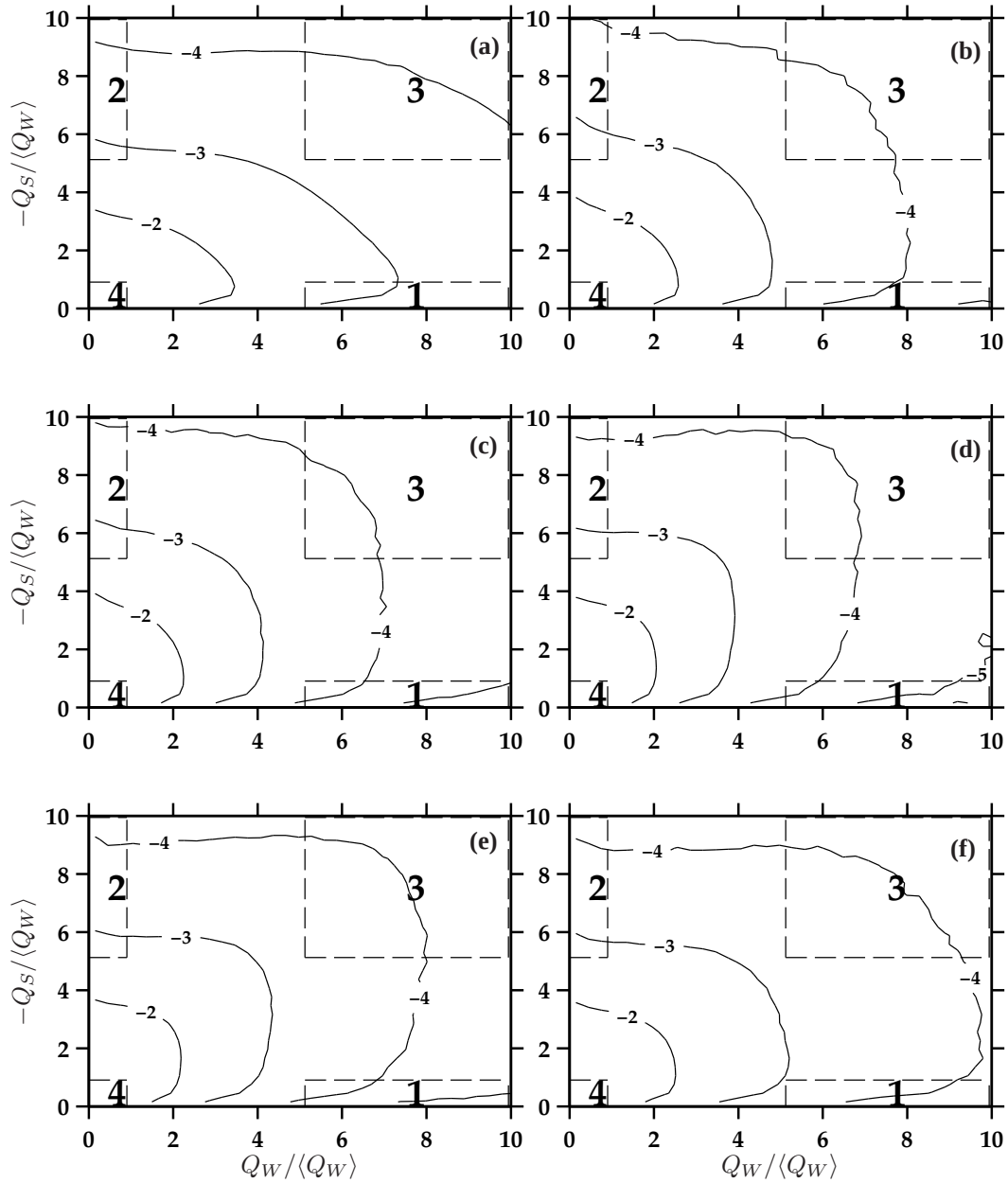

Figure 2. Joint PDF of the invariant pair $(Q_W, -Q_S)$ for (a) $St = 0.0$, (b) $St = 0.1$, (c) $St = 0.2$, (d) $St = 0.5$, (e) $St = 1$, and (f) $St = 2$. The areas outlined by dashed lines correspond to 1 - high Q_W and low Q_S, 2 - high Q_S and low Q_W, 3 - high Q_W and high Q_S, and 4 - low Q_W and low Q_S. The exponents of the decade are indicated on the contour lines.

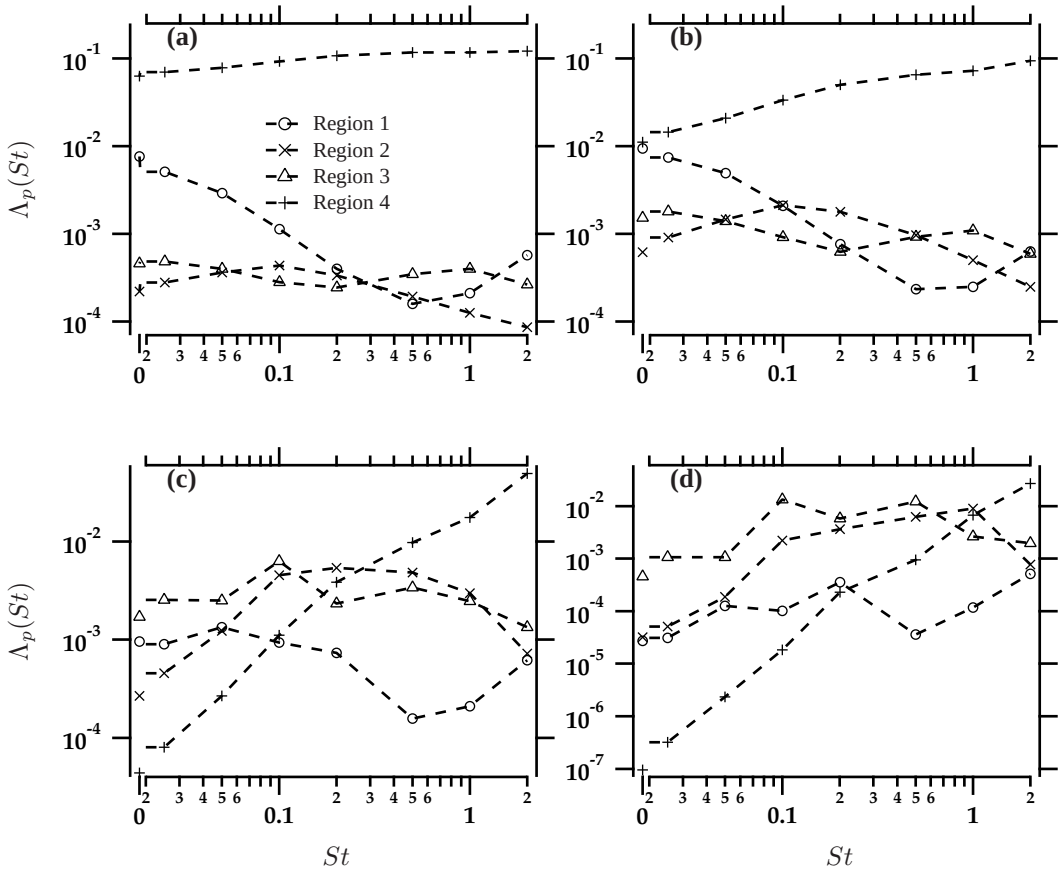

Figure 3. Contribution of the regions outlined in the $(Q_W, -Q_S)$ plane of Figures 1 and 2 to higher-order acceleration moments for (a) $p = 2$, (b) $p = 4$, (c) $p = 6$, and (d) $p = 8$.

4. CONCLUSIONS

In order to better understand how acceleration is related to flow topology, we compute invariants of the strain-rate and rotation-rate tensor along particle trajectories. The joint PDFs of invariant pairs along with acceleration contour plots on invariant planes allow us to compute the contribution of specific flow topologies to the acceleration moments. We find further confirmation that inertial particles are ejected from regions of high-rotation and that these contribute the least to the acceleration moments precisely as clustering or preferential concentration peaks at $St \approx 0.7$. We believe this work will contribute to a better understanding of the effects of inertia on acceleration and how flow topology relates to the latter.

5. REFERENCES

Bec, J., Biferale, L., Boffetta, G., Celani, A., Cencini, M., Lanotte, A.S., Musacchio, S. and Toschi, F., 2006. "Acceleration statistics of heavy particles in turbulence". *J. Fluid Mech.*, Vol. 550, pp. 349–358.

Brown, R.D., Warhaft, Z. and Voth, G.A., 2009. "Acceleration statistics of neutrally buoyant spherical particles in intense turbulence". *Phys. Rev. Lett.*, Vol. 103, p. 194501.

Brucker, K.A., Isaza, J.C., Vaithianathan, T. and Collins, L.R., 2007. "Efficient algorithm for simulating homogeneous turbulent shear flow without remeshing". *J. Comp. Phys.*, Vol. 225, pp. 20–32.

Calzavarini, E., Volk, R., Bourgoin, M., Leveque, E., Pinton, J.F. and Toschi, F., 2009. "Acceleration statistics of finite-sized particles in turbulent flow: the role of Faxen forces". *J. Fluid Mech.*, Vol. 630, pp. 179–189.

Cantwell, B.J., 1992. "Exact solution of a restricted Euler equation for the velocity-gradient tensor". *Phys. Fluids A*, Vol. 4, No. 4, pp. 782–793.

Chong, M.S., Perry, A.E. and Cantwell, B.J., 1990. "A general classification of three-dimensional flow fields". *Phys. Fluids A*, Vol. 2, No. 5, pp. 765–777.

da Silva, C.B. and Pereira, J.C.F., 2008. "Invariants of the velocity-gradient, rate-of-strain, and rate-of-rotation tensors across the turbulent/nonturbulent interface in jets". *Phys. Fluids*, Vol. 20, No. 5, p. 055101.

Gerashchenko, S., Sharp, N.S., Neuscamman, S. and Warhaft, Z., 2008. "Lagrangian measurements of inertial particle accelerations in a turbulent boundary layer". *J. Fluid Mech.*, Vol. 617, pp. 255–281.

Gylfason, A., Ayyalasomayajula, S. and Warhaft, Z., 2004. "Intermittency, pressure and acceleration statistics from hot-wire measurements in wind-tunnel turbulence". *J. Fluid Mech.*, Vol. 501, pp. 213–229.

Lavezzo, V., Soldati, A., Gerashchenko, S., Warhaft, Z. and Collins, L.R., 2010. "On the role of gravity and shear on the acceleration of inertial particles in near-wall turbulence". *J. Fluid Mech.* Accepted for publication.

Maxey, M.R. and Riley, J.J., 1983. "Equation of motion for a small rigid sphere in a nonuniform flow". *Phys. Fluids*, Vol. 26, pp. 883–889.

Mordant, N., Crawford, A.M. and Bodenschatz, E., 2004. "Experimental Lagrangian acceleration probability density function measurement". *Physica D*, Vol. 193, pp. 245–251.

Pope, S.B., 1994. "Lagrangian PDF methods for turbulent flows". *Annu. Rev. Fluid Mech.*, Vol. 26, pp. 23–63.

Pope, S.B., 2002. "A stochastic Lagrangian model for acceleration in turbulent flows". *Phys. Fluids*, Vol. 14, pp. 2360–2375.

Qureshi, N.M., Arrieta, U., Baudet, C., Cartellier, A., Gagne, Y. and Bourgoin, M., 2008. "Acceleration statistics of inertial particles in turbulent flow". *Eur. Phys. J. B*, Vol. 66, No. 4, pp. 531–536.

Salazar, J.P.L.C. and Collins, L.R., 2009. "Two-particle dispersion in isotropic turbulent flows". *Annu. Rev. Fluid Mech.*, Vol. 41, pp. 405–432.

Soria, J., Sondergaard, R., Cantwell, B.J., Chong, M.S. and Perry, A.E., 1994. "A study of the fine-scale motions of incompressible time-developing mixing layers". *Phys. Fluids*, Vol. 6, No. 2, pp. 871–884.

Sundaram, S. and Collins, L.R., 1997. "Collision statistics in an isotropic, particle-laden turbulent suspension I. Direct

numerical simulations". *J. Fluid Mech.*, Vol. 335, pp. 75–109.

Volk, R., Calzavarini, E., Verhille, G., Lohse, D., Mordant, N., Pinton, J.F. and Toschi, F., 2008. "Acceleration of heavy and light particles in turbulence: Comparison between experiments and direct numerical simulations". *Physica D-Nonlinear Phenomena*, Vol. 237, pp. 2084–2089.

Xu, H. and Bodenschatz, E., 2008. "Motion of inertial particles with size larger than Kolmogorov scale in turbulent flows". *Physica D*, Vol. 237, pp. 2095–2100.

Yeung, P.K., Pope, S.B., Kurth, E.A. and Lamorgese, A.G., 2007. "Lagrangian conditional statistics, acceleration and local relative motion in numerically simulated isotropic turbulence". *J. Fluid Mech.*, Vol. 582, pp. 399–422.

Yeung, P.K., Pope, S.B., Lamorgese, A.G. and Donzis, D.A., 2006a. "Acceleration and dissipation statistics of numerically simulated isotropic turbulence". *Phys. Fluids*, Vol. 18, No. 6, p. 065103.

Yeung, P.K., Pope, S.B. and Sawford, B.L., 2006b. "Reynolds number dependence of Lagrangian statistics in large numerical simulations of isotropic turbulence". *J. Turbulence*, Vol. 7, No. 58, pp. 1–12.

6. RESPONSIBILITY NOTICE

The authors are the only responsible for the printed material included in this paper.